C. R. Chimie 21 (2018) 669–675

Contents lists available at ScienceDirect

Comptes Rendus Chimie

www.sciencedirect.com

Full paper/Mémoire

Theoretical study of Sn adsorbed on the MgO(100) surface with defects

Piotr Matczak

Department of Physical Chemistry, Faculty of Chemistry, University of Łódź, Pomorska 163/165, 90-236 Lodz, Poland

ARTICLE INFO

Article history:
Received 11 November 2017
Accepted 15 March 2018
Available online 13 April 2018

Keywords:
Adsorption
Tin
Magnesium oxide
DFT calculations

ABSTRACT

In this study, the adsorption of Sn atom at various sites on the MgO(100) surface was characterized using a theoretical approach based on density functional theory calculations. Both regular adsorption centers (O^{2-} and Mg^{2+}) and defects (such as neutral and charged O and Mg vacancies) were considered. Several key parameters for these sites with the adsorbed Sn atom were determined to provide its geometric, energetic, and electronic characterization. The interaction between Sn and the Mg vacancy sites is very strong and is associated with a relatively small distance of the adsorbed Sn atom from the surface and with a large electronic charge transfer from Sn to the surface. A much smaller strength of Sn atom adsorption is observed for the O vacancies and regular sites. Among them, the F_s^0 center binds the Sn atom strongest and, in consequence, this atom acquires a significant amount of electronic charge.

1. Introduction

Magnesium oxide (MgO) plays an important role in heterogeneous catalysis [1,2]. Its single crystal (100) surface has received a great deal of attention because this surface itself is catalytically active toward some reactions [2–4], and in addition, it can serve as a substrate for supported metal catalysts [5–9]. The (100) face is more stable in terms of its surface energy than other faces of MgO [10,11]. It is also easy to prepare [12] and possesses well-defined stoichiometry and a simple rock-salt structure that does not exhibit any significant relaxation [13,14]. Due to these features, MgO(100) constitutes a useful model surface for fundamental studies of supported metal catalysts [15]. On an MgO(100) single crystal there are always surface defects (ca. 10^{12}–10^{13} defects/cm^2) [16] that modify catalytic properties of both the surface and adsorbed metals [17]. For instance, some surface point defects, such as oxygen vacancies, trap electronic charge and thus can promote catalytic reactions through electron transfer [18]. Furthermore, it is known that metals deposited on MgO exhibit diverse catalytic properties, depending on the kind of adsorption site, whether it is a regular site or a defect [19–21].

In the field of heterogeneous catalysis, catalysts containing tin deposited on MgO have found applications in the selective hydrogenation of α,β-unsaturated aldehydes [22] and the selective dehydrogenation of alkanes [23,24]. In these catalysts, platinum is doped with tin to introduce desired promoting effects [25]. Tin in the Pt–Sn/MgO catalysts suppresses side reactions on the support surface and inhibits Pt particle sintering [22]. It is known that the activity of the Pt–Sn catalyst in butadiene hydrogenation is lower than that of the Pt catalyst but the former is more selective toward the formation of butenes, which is industrially important [26]. The presence of Sn in a catalyst may also open a new reaction path, as it happens for benzene production from acetylene on Sn/Pt(111) [27]. A promising application of tin-modified Pt catalysts for the electrooxidation of CO, formaldehyde, formic acid, and methanol was also reported [28].

E-mail addresses: piotr.matczak@chemia.uni.lodz.pl, p.a.matczak@gmail.com.

https://doi.org/10.1016/j.crci.2018.03.005
1631-0748/

A microscopic view of metal adsorption on MgO(100) can be easily obtained from electronic structure methods based on density functional theory (DFT) [17,29]. Such methods are capable of (1) providing an electronic description of adsorption sites and (2) estimating the strength of metal–surface interactions. There are plenty of theoretical studies in which DFT calculations have been carried out to characterize metal adsorption on MgO(100), for example, Refs. [30–47]. Most of these studies are focused on the adsorption of transition metal atoms [30–44]. As compared to the large number of theoretical studies devoted to the adsorption of Pt on MgO(100) [30,32,33,37,39,40,42], little attention has been paid to the theoretical characterization of Sn adsorption on this surface. To our knowledge, one theoretical study dealing with Sn/MgO(100) is available [48]. In this study, molecular dynamics calculations were performed to simulate the wetting behavior of liquid tin on MgO(100). Similarly, there have been merely a few efforts devoted to the theoretical examination of Sn adsorption on other oxides, such as CeO_2(111) [49], Fe_3O_4(100) [50], and γ-Al_2O_3(110) [51].

The aforementioned distinct lack of electronic structure investigations of Sn/MgO(100) has encouraged us to perform DFT calculations for a series of model systems simulating a Sn atom adsorbed at various sites on the MgO(100) surface. Both regular sites (O^{2-} and Mg^{2+} surface adsorption centers) and defective sites (such as neutral and charged O and Mg surface vacancies) are taken into account. Geometric, energetic, and electronic properties of the Sn atom adsorbed at these sites are calculated in this study to characterize Sn adsorption on MgO(100) at the atomic level.

2. Computational methods

The applied computational methodology makes use of the B3LYP hybrid density functional [52–54], which has been successfully used to study metal adsorption on MgO(100) [34,35,38,39,41,42]. This functional is combined with the DFT-D3(BJ) empirical dispersion correction [55,56] to account for dispersion interactions. In a recent study of N_2O adsorption on MgO(100) [57], it was shown that this correction performed better than other kinds of Grimme's dispersion corrections proposed for B3LYP (the choice of dispersion correction is discussed further in Section S2 of Supporting Information). The regular and defective adsorption sites on MgO(100) are simulated by means of respective embedded cluster models (details can be found in Section S1 of Supporting Information). In short, stoichiometric two-layer clusters $Mg_{13}O_{13}$ are used to represent the surface O^{2-} and Mg^{2+} centers (see Fig. 1). These clusters possess the structure of an ideal MgO crystal lattice. Clusters simulating the defective sites are formed by removing the central atom or ion from the surface layer of the $Mg_{13}O_{13}$ clusters. The removal of O, O^-, O^{2-}, Mg, Mg^+, or Mg^{2+} produces a center labeled as F_s^0, F_s^+, F_s^{2+}, V_s^0, V_s^-, or V_s^{2-}, respectively (see Table 1). These labels are widely used to classify point defects on MgO [17,18]. Their superscripts indicate the formal charge of a defect, whereas their subscripts refer to defect location on the surface. All the clusters are embedded in a large array of ±2 point charges placed at the positions of an ideal MgO lattice. The positive point charges at the boundary with the clusters are replaced by total ion model potentials. A single Sn atom is adsorbed in the center of the clusters and the perpendicular distance from the Sn atom to the surface layer of clusters is optimized. During the Sn adsorption, the Mg and O atoms directly interacting with Sn are allowed to relax, whereas more distant Mg and O atoms are kept frozen. Further in this study, the denotation "Sn/site" refers to a structure with its Sn atom adsorbed at a given site on MgO(100).

For all considered clusters, their Mg and O atoms directly involved in the interaction with the Sn atom are described by the 6-31+G(d) basis set [58–60]. These atoms are surrounded by Mg and O treated with 6-31G(d). The 6-31G basis set is ascribed to the Mg and O atoms that are most distant from each adsorption center. The suitability of such a mixed basis set scheme for modeling MgO(100) by means of cluster models was confirmed in several previous works [61–63]. The total ion model potentials use the LANL2 effective core potential of Mg^{2+} [64]. The LANL08d

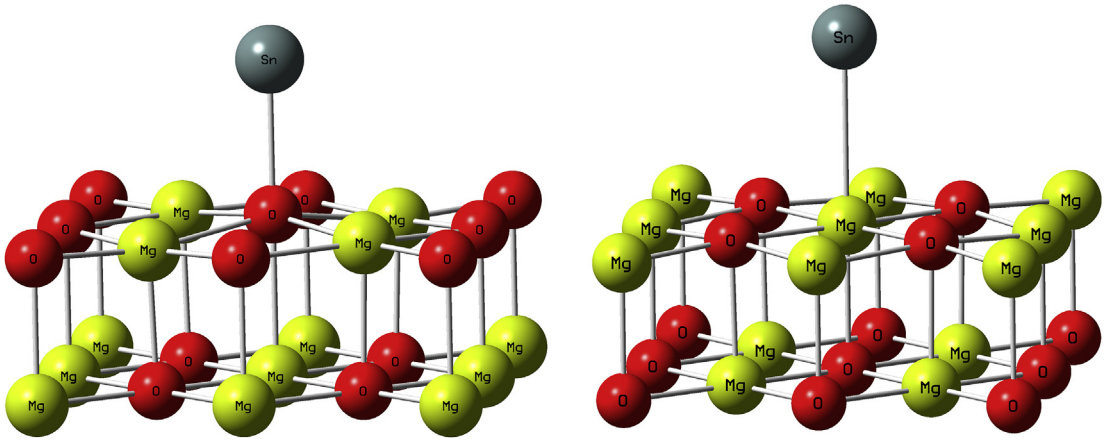

Fig. 1. $Mg_{13}O_{13}$ clusters used in the models representing the O^{2-} (left) and Mg^{2+} (right) centers. Optimized structures of the clusters with the adsorbed Sn atom are shown.

Table 1
Summary of the nomenclature used to identify the regular and defective sites on MgO(100).

Label	Description
O^{2-}	Five-coordinated surface O^{2-} anion
Mg^{2+}	Five-coordinated surface Mg^{2+} cation
F_s^0	Missing surface O atom. Two electrons are trapped at this site
F_s^+	Missing surface O^- anion. One electron is trapped at this site
F_s^{2+}	Missing surface O^{2-} anion
V_s^0	Missing surface Mg atom. Two electron holes are associated with this site
V_s^-	Missing surface Mg^+ cation. One electron hole is associated with this site
V_s^{2-}	Missing surface Mg^{2+} cation

basis set is assigned to the Sn atom [65]. This basis set includes 1p1d polarization functions [66].

Two electronic states are considered for each surface site with the Sn atom adsorbed. One is a low-spin state that corresponds to either a singlet (for Sn/O^{2-}, Sn/Mg^{2+}, Sn/F_s^0, Sn/F_s^{2+}, Sn/V_s^0, and Sn/V_s^{2-}) or doublet configuration (for Sn/F_s^+ and Sn/V_s^-). The second is a high-spin state that is assumed to exhibit either a quartet (for Sn/F_s^+ and Sn/V_s^-) or triplet multiplicity (for Sn at the rest of adsorption centers).

The adsorption energy E_{ads} of a single Sn atom at a given site is defined as

$$E_{ads} = E_{tot}(Sn/site) - E_{tot}(Sn) - E_{tot}(site)$$

where $E_{tot}(Sn/site)$ is the total energy of the Sn/site structure, $E_{tot}(Sn)$ is the energy of the isolated Sn atom, and $E_{tot}(site)$ is the energy of embedded cluster simulating a given adsorption site. If $E_{tot}(site)$ is calculated for the geometry taken from the Sn/site structure, the binding energy E_{bin} is obtained. E_{bin} for the low-spin structures assumes the singlet multiplicity of Sn. Although E_{ads} evaluates the energetic effect associated with the formation of a Sn/site structure from its isolated constituents, E_{bin} estimates the strength of Sn–site interaction for the Sn/site structure. The E_{bin} energies reported in this study are counterpoise corrected [67]. The charge q and spin density acquired by the Sn atom adsorbed at the investigated centers are expressed in terms of the Bader topological analysis of electron density [68].

Gaussian 09 D.01 software [69] has been used to carry out all computations except the Bader analysis calculations that have been done with the Multiwfn 3.4 program [70].

3. Results and discussion

Table 2 presents essential geometric and energetic parameters describing the Sn atom adsorption at the studied sites. It is evident that the Sn atom prefers being adsorbed at the O^{2-} center on the nondefective MgO(100) surface. The corresponding E_{ads} values clearly indicate the existence of a thermodynamic force toward the formation of Sn/O^{2-} structure. In contrast, the occurrence of Sn/Mg^{2+} is associated with a very small energetic effect. Only this structure in its high-spin state can be formed in an exothermic process ($E_{ads} < 0$). The comparison of E_{ads} obtained from B3LYP-D3(BJ) and B3LYP reveals that the favorable effect of adsorption for Sn/Mg^{2+} in the high-spin state is attributed almost entirely to dispersion interactions. The strong preference of the Sn atom to adsorb at the O^{2-} center rather than at the Mg^{2+} center is also reflected by the distance of the adsorbed Sn atom from each center (see $d_{Sn-surf}$ in Table 2). As a matter of fact, both Sn/Mg^{2+} structures are characterized by large values of $d_{Sn-surf}$.

From the values of the relative total energy ΔE shown in Table 2, it is clear that the Sn atom adsorption at the O^{2-} and Mg^{2+} centers tends to conserve the high-spin state of Sn (its ground state exhibits a triplet configuration). The E_{ads} values of Sn/O^{2-} in both the high- and low-spin states are negative but the formation of Sn/O^{2-} in the high-spin state is thermodynamically more favorable. The formation of Sn/Mg^{2+} does not provide a sufficient energy for spin pairing in Sn ($E_{ads} > 0$ in the low-spin state).

Table 2
Distance between Sn and the surface ($d_{Sn-surf}$), relative total energy (ΔE), adsorption energy (E_{ads}), and binding energy (E_{bin}) for the Sn/site structures in their low- and high-spin states.[a]

Sn/site	Spin state	$d_{Sn-surf}$	ΔE	E_{ads}	E_{bin}
Sn/O^{2-}	Low	2.418 (2.422)	0.82 (0.81)	−1.11 (−0.49)	−2.27 (−1.65)
	High	2.422 (2.436)	0.00 (0.00)	−1.93 (−1.30)	−2.02 (−1.40)
Sn/Mg^{2+}	Low	2.985 (3.171)	0.77 (0.89)	0.27 (0.82)	−0.72 (−0.16)
	High	3.146 (3.524)	0.00 (0.00)	−0.50 (−0.07)	−0.52 (−0.02)
Sn/F_s^0	Low	2.207 (2.274)	0.73 (0.72)	−2.32 (−1.65)	−3.29 (−2.62)
	High	2.209 (2.278)	0.00 (0.00)	−3.05 (−2.37)	−2.97 (−2.30)
Sn/F_s^+	Low	2.359 (2.356)	0.19 (0.17)	−1.90 (−1.25)	−2.78 (−2.13)
	High	2.317 (2.324)	0.00 (0.00)	−2.09 (−1.42)	−2.04 (−1.35)
Sn/F_s^{2+}	Low	2.308 (2.571)	0.15 (0.24)	−1.26 (−0.51)	−2.25 (−1.50)
	High	2.328 (2.702)	0.00 (0.00)	−1.41 (−0.75)	−1.34 (−0.71)
Sn/V_s^0	Low	0.840 (0.909)	0.00 (0.00)	−11.17 (−10.06)	−12.11 (−11.17)
	High	0.366 (0.427)	2.33 (2.45)	−8.84 (−7.61)	−10.21 (−9.15)
Sn/V_s^-	Low	0.843 (0.892)	0.00 (0.00)	−8.56 (−7.56)	−9.99 (−9.03)
	High	0.378 (0.418)	1.79 (1.93)	−6.77 (−5.63)	−7.78 (−6.72)
Sn/V_s^{2-}	Low	0.809 (0.874)	0.00 (0.28)	−8.00 (−6.99)	−9.82 (−8.85)
	High	0.827 (0.870)	0.03 (0.00)	−7.97 (−7.27)	−8.86 (−8.17)

[a] $d_{Sn-surf}$ are presented in Å and all energies are presented in eV. For each kind of the adsorption site, ΔE are calculated relative to the energy of the structure possessing the lowest total energy. Results obtained from B3LYP calculations are given in parentheses.

The strong preference of Sn/O^{2-} over Sn/Mg^{2+} is in line with the findings made for the adsorption of transition metal atoms on MgO(100) [31,71,72]. Moreover, it was reported that the interaction between Mg^{2+} centers and several second-row transition metal atoms, such as Pd and Ag, was virtually zero [31]. The E_{ads} value of −1.93 eV for Sn/O^{2-} in the high-spin state indicates that the adsorption of Sn at the O^{2-} center is more exothermic than that of many transition metals at this center [31,73].

The Sn atom adsorption is energetically favorable for all studied defective sites. For three O vacancy sites, the E_{ads} values vary in the order $F_s^0 < F_s^+ < F_s^{2+}$, which indicates that the formation of Sn/F_s^0 structure is thermodynamically preferred. The favorable energetic effects of the Sn-atom adsorption at F_s^0 and F_s^+ are larger in magnitude than E_{ads} for Sn/O^{2-}. In this regard, the F_s^0 and F_s^+ centers contrast with F_s^{2+} where the adsorption of the Sn atom in the high-spin state turns out to be less likely than at the O^{2-} center. This is obviously illustrated by the less negative E_{ads} value of the high-spin Sn/F_s^{2+} structure as compared to E_{ads} for Sn/O^{2-} in its high-spin state. Another reason for the little likelihood of Sn/F_s^{2+} formation is the low density of F_s^{2+} centers on MgO(100), which is due to their high formation energy [74]. The F_s^0 centers constitute the majority of oxygen vacancies created by the electron bombardment of MgO(100) [18,75]. A stronger thermodynamic force toward adsorption at F_s^0 rather than at O^{2-} was previously detected for several first- and second-row transition metals (Co, Ni, Cu, Pd, and Ag) [31,73]. Moreover, the adsorption of Sn at F_s^0 produces a more exothermic effect than the adsorption of all first-row transition metals, except Ni, at this center [73]. The Sn atom shows highly energetic adsorption at three Mg vacancy sites, with the E_{ads} values falling in the range from −6.77 to −11.17 eV. These values are many times greater in magnitude than E_{ads} calculated for two regular and three O vacancy sites. Consequently, it can be inferred from E_{ads} that on the defective MgO(100) surface the Sn atom preferentially sits at three Mg vacancy sites, in particular at the V_s^0 center. It should be noted, however, that the concentration of surface Mg vacancy sites is probably lower than that of O vacancies on MgO(100). According to an electron energy loss spectroscopy study of MgO(100) growth on Ag(100), it has been suggested that Mg vacancies may not be as abundant as O vacancies [76]. It is known from theoretical studies [74,77] that the formation energy of V_s^0 centers on MgO(100) is very high, larger than that of F_s^0. This seems to be in line with the low density of Mg vacancies on the MgO(100) surface. The comparison of $d_{Sn–surf}$ for all defective sites reveals that the Sn atom is particularly close to the surface upon its adsorption at the Mg vacancy sites.

As evidenced by the ΔE values in Table 2, the high-spin states of Sn/F_s^0, Sn/F_s^+, and Sn/F_s^{2+} are more stable than their low-spin counterparts. In other words, the Sn atom adsorbed at the F_s^0, F_s^+, or F_s^{2+} center tends to maintain its atomic spin state. On the other hand, the low-spin states of Sn/V_s^0 and Sn/V_s^- are thermodynamically favored. This results in quenching the magnetic moment of Sn adsorbed at V_s^0 and V_s^-. For an isolated Sn atom, its transition energy from a triplet to a singlet requires 0.99 eV at the B3LYP/LANL08d level of theory. Because the stabilization of Sn/V_s^0 in its low-spin state amounts to 2.33 eV, this is large enough to quench the spin state to a singlet. Similarly, the stabilization of the low-spin Sn/V_s^- structure provides enough energy to reach partial coupling between unpaired electrons. It is worth reminding that the ground state of V_s^0 center is a triplet [77], which fosters coupling unpaired electrons from Sn and V_s^0. The comparison of ΔE with the triplet–singlet transition energy of an isolated Sn atom reveals that the adsorption sites favoring the high-spin state of Sn induce a decrease in the transition energy (ΔE < 0.99 eV). An analogous decrease in the energy required to reach a low-spin state was previously observed for many first-row transition metal atoms adsorbed at O^{2-} and F_s^0 [43]. In the case of Sn/V_s^{2-}, its low- and high-spin states lie too close to one another to designate the preferred spin state unambiguously.

The strength of the interaction between Sn and each adsorption site in the studied Sn/site structures can be estimated by E_{bin}, as shown in Table 2. The values of E_{bin} are well correlated with the E_{ads} values; the correlation between E_{bin} and E_{ads} is characterized by the coefficient of determination $R^2 = 0.984$. Therefore, trends in E_{bin} mimic those discussed above for E_{ads}. In particular, E_{bin} correlates inversely with $d_{Sn–surf}$ (see Fig. 2). As the strength of Sn–site interaction increases, the corresponding Sn–surface distance decreases. By comparing E_{bin} with E_{ads}, it is possible to evaluate an effect associated with the structural relaxation of surface centers upon Sn atom adsorption. It is particularly straightforward for the Sn/site structures in their high-spin states because in such cases the difference between E_{bin} and E_{ads} can be entirely attributed to this effect. E_{bin} does not differ much from E_{ads} for two regular and three O vacancy sites, which implies a rather minor relaxation of these sites upon the formation of high-spin Sn/site structures. In addition, the relaxation of adsorption sites can obviously be expressed in terms of their geometrical parameters. Table 3 presents displacements Δd in the positions of atoms belonging to the surface layer of each studied adsorption site. For the high-spin Sn/O^{2-} and Sn/

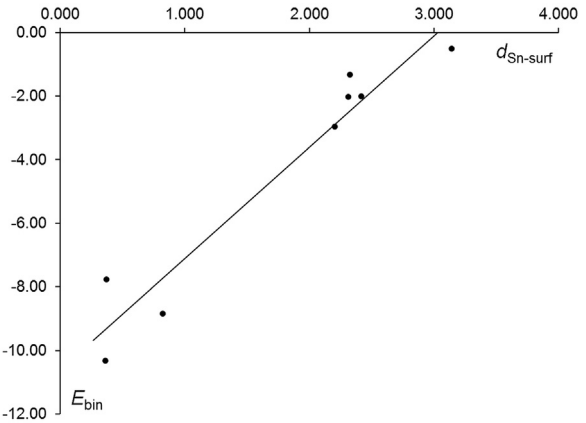

Fig. 2. Binding energies (E_{bin} in eV) versus distances between Sn and the MgO(100) surface ($d_{Sn–surf}$ in Å) for all studied Sn/site structures in their high-spin states.

Table 3
Displacements (Δd) in the positions of atoms in the surface layer of adsorption sites for the Sn/site structures in their low- and high-spin states.[a]

Sn/site	Spin state	Δd_x(O)	Δd_x(Mg_4)	Δd_{yz}(Mg_4)	Δd_x(Mg)	Δd_x(O_4)	Δd_{yz}(O_4)
Sn/O^{2-}	Low	0.171	−0.026	−0.074			
	High	0.154	0.019	−0.068			
Sn/Mg^{2+}	Low				−0.021	−0.003	−0.005
	High				0.121	0.023	−0.024
Sn/F_s^0	Low		0.029	−0.071			
	High		0.028	−0.053			
Sn/F_s^+	Low		−0.025	−0.008			
	High		0.037	−0.034			
Sn/F_s^{2+}	Low		−0.032	0.040			
	High		0.018	0.024			
Sn/V_s^0	Low					0.049	0.134
	High					−0.011	0.207
Sn/V_s^-	Low					0.010	0.163
	High					−0.020	0.230
Sn/V_s^{2-}	Low					0.007	0.186
	High					−0.010	0.202

[a] All displacements are presented in Å. Δd are calculated relative to the structures of isolated adsorption centers.

Mg^{2+} structures, their O^{2-} or Mg^{2+} atom beneath the adsorbed Sn atom is moved vertically upward, that is, in the direction normal to the surface. The corresponding displacements Δd_x are below 0.2 Å, and they are qualitatively similar to those observed for the adsorption of many transition metal atoms [37]. The adsorption of Sn at three O vacancy sites results in small or even negligible displacements of four Mg atoms surrounding each O vacancy. This is the reason for the very small differences between E_{bin} and E_{ads} for Sn/F_s^0, Sn/F_s^+, and Sn/F_s^{2+} in their high-spin states. The Sn atom adsorption at three Mg vacancy sites more noticeably affects the structure of these sites. In particular, four O atoms surrounding each Mg vacancy in the surface layer show a lateral shift: they are moved outward in the surface plane ($\Delta d_{yz}(O_4) > 0$). This structural rearrangement greatly contributes to the difference between E_{bin} and E_{ads} for Sn/V_s^0, Sn/V_s^-, and Sn/V_s^{2-} in their high-spin states.

The vast majority of the studied Sn/site structures shows the $d_{Sn–surf}$ distances that are only marginally affected by the inclusion of dispersion correction into B3LYP calculations. A more evident effect of dispersion correction on $d_{Sn–surf}$ can be observed for Sn/Mg^{2+} and Sn/F_s^{2+}. In the case of the former, this can be easily explained by the fact that the Sn—site interaction in Sn/Mg^{2+} is very weak and governed by dispersion forces. The effect of dispersion correction on E_{bin} for Sn adsorbed at three Mg vacancy sites does not exceed 15%. For the O^{2-} and three O vacancy sites, the dispersion correction causes a strengthening in the Sn—site interaction, amounting up to 50%. Unsurprisingly, the effect of dispersion correction is greatest for E_{bin} in Sn/Mg^{2+}.

An important factor determining the reactivity of metal atoms adsorbed on a surface is the amount of electronic charge acquired by these atoms [78–80]. This charge results from the electron redistribution between the atoms and the surface, which is sensitive to their interaction. For each Sn/site structure, the partial atomic charge of Sn was calculated and the resulting q values are listed in Table 4. These q values may also be regarded as an approximate indication of charge transfers between Sn and the adsorption sites. Accordingly, a very limited charge transfer between the Sn atom and the O^{2-} center is observed for both Sn/O^{2-} structures. In this respect, the Sn atom adsorption is not very different from the adsorption of transition metal atoms at the O^{2-} center [37]. The Sn atom behaves as a weak electron acceptor when adsorbed at O^{2-}. However, it remains essentially neutral at the Mg^{2+} center, reflecting the weakness of Sn—Mg^{2+} interaction. Similarly to Sn/O^{2-}, the Sn/F_s^0 and Sn/F_s^+ structures demonstrate charge transfers from the adsorption sites to the Sn atom. The charge transfer is particularly pronounced for Sn/F_s^0. This is expected because the F_s^0 vacancy possesses two extra electrons that are largely localized in the center of this vacancy, whereas the F_s^+ vacancy has only one extra electron [74]. Moreover, Sn/F_s^0 is characterized by a larger charge transfer than Sn/O^{2-} because the two extra electrons of F_s^0 are more polarizable than those of the surface O^{2-} anion. The direction of charge transfer is reversed for Sn/F_s^{2+} and the Sn atom donates ca. 0.05 electron to the F_s^{2+} center. This direction is in agreement with the

Table 4
Charge (q) and spin density for the Sn atom in the low- and high-spin Sn/site structures.[a]

Sn/site	Spin state	q	Spin density
Sn/O^{2-}	Low	−0.113	0.000
	High	−0.109	1.724
Sn/Mg^{2+}	Low	−0.015	0.000
	High	−0.012	1.818
Sn/F_s^0	Low	−1.405	0.000
	High	−1.417	1.680
Sn/F_s^+	Low	−0.653	0.885
	High	−0.665	2.425
Sn/F_s^{2+}	Low	0.052	0.000
	High	0.048	1.632
Sn/V_s^0	Low	1.337	0.000
	High	1.893	0.600
Sn/V_s^-	Low	1.334	0.008
	High	1.883	0.604
Sn/V_s^{2-}	Low	1.327	0.000
	High	1.310	0.014

[a] All values are presented in atomic units.

tendency of F_s^{2+} to accept electronic charge and to form a more stable F_s^{+} center [74]. Table 4 also presents the spin density on the Sn atom in the Sn/site structures. The spin density values for Sn adsorbed at two regular and three O vacancy sites indicate that their respective high-spin Sn/site structures exhibit the spin density concentrated mainly on the Sn atom. The adsorption of Sn at three Mg vacancy sites leads to a reduction in the electronic charge of Sn. The magnitude of this reduction decreases in the order $Sn/V_s^0 > Sn/V_s^- > Sn/V_s^{2-}$. The great charge transfer from Sn to V_s^0 results from the strong electron-deficient character of the V_s^0 center. The three Mg vacancy sites are able to ionize the Sn atom, which loses at least 1.3 electrons. This finding agrees in part with previous results reported for the adsorption of Rb, Pd, and Ag atoms [31]. These atoms formed a (di)cation at the V_s^0 and V_s^- centers but not at the V_s^{2-} center. Furthermore, the Pd^{2+} cation practically replaced the missing Mg^{2+} cation of the V_s^0 site. For the high-spin Sn/V_s^0 and Sn/V_s^- structures, their $d_{Sn-surf}$ distances are indeed very short yet not short enough to insert the Sn atom into the cavity of the V_s^0 or V_s^- site. The ionization of the Sn atom by the Mg vacancy sites leads to the occurrence of a strong electrostatic stabilization effect. The occurrence of such an effect is supported by the significant magnitude of the corresponding E_{bin} values. The spin density in the high-spin Sn/V_s^0, Sn/V_s^-, and Sn/V_s^{2-} structures is distributed, to a large extent, inside and around the vacancies. In consequence, the spin density values for the Sn atom in these structures are much smaller than those of Sn adsorbed at three O vacancy sites. An extreme spin delocalization toward the adsorption site is detected for the high-spin Sn/V_s^{2-} structure. Although the spin multiplicity of the low-spin Sn/V_s^- structure is a doublet, the spin density value for its Sn atom is almost equal to zero. This implies that the magnetic moment of Sn in the low-spin Sn/V_s^- structure is practically quenched.

4. Conclusions

In this study, the adsorption of Sn at various nondefective and defective sites on the MgO(100) surface has been characterized at the atomic level, using a theoretical approach based on the B3LYP-D3(BJ) density functional and embedded cluster models of the surface. Of the considered nondefective adsorption sites, the Sn atom preferably occupies the O^{2-} center, with not very large adsorption energy, on the order of 1–2 eV. The energetic effects of the Sn-atom adsorption at the F_s^0, F_s^+, and F_s^{2+} centers do not differ much from that of Sn/O^{2-}. In contrast to the three O vacancy centers, the Mg vacancy sites bind the Sn atom very strongly, with the corresponding adsorption energies ranging from ca. −7 to −11 eV. The stability of spin states for the Sn/site structures is usually governed by Hund's rule, which favors the high-spin multiplicity of the adsorbed atom. Only the Sn/V_s^0 and Sn/V_s^- structures, for which the strength of Sn–site interaction is greatest, tend to reduce the number of their unpaired electrons. The magnitude of electronic charge acquired by the Sn atom upon adsorption depends heavily on the kind of adsorption site. The Sn atom adsorbed at the F_s^0 and F_s^+ centers accepts a large amount of electronic charge, whereas a considerable charge transfer from Sn to the surface is observed for three Mg vacancy sites.

We hope that the presented characterization of a single Sn atom adsorbed at various sites on MgO(100) may be an important step toward understanding many processes involving Sn and MgO(100), for example, the nucleation of Sn nanoparticles on this surface. Furthermore, this characterization is an essential prerequisite for the future investigation of reactions activated by catalysts containing Sn deposited on MgO.

Acknowledgments

This work was partially supported by PL-Grid Infrastructure.

Appendix A. Supplementary data

Supplementary data related to this article can be found at https://doi.org/10.1016/j.crci.2018.03.005.

References

[1] V.E. Henrich, P.A. Cox, The Surface Science of Metal Oxides, Cambridge University Press, Cambridge, UK, 1994.
[2] J.I. Di Cosimo, V.K. Diez, C. Ferretti, C.R. Apesteguia, in: J. Spivey, K.M. Dooley, Y.-F. Han (Eds.), Catalysis, The Royal Society of Chemistry, Cambridge, UK, 2014, pp. 1–28.
[3] C. Xu, B.E. Koel, J. Chem. Phys. 102 (1995) 8158–8166.
[4] X.D. Peng, M.A. Barteau, Catal. Lett. 7 (1990) 395–402.
[5] Y.C. Lee, P. Tong, P.A. Montano, Surf. Sci. 181 (1987) 559–572.
[6] E. Ruckenstein, Y.H. Hu, Appl. Catal. A 154 (1997) 185–205.
[7] B.-Q. Xu, J.-M. Wei, H.-Y. Wang, K.-Q. Sun, Q.-M. Zhu, Catal. Today 68 (2001) 217–225.
[8] F. Frusteri, S. Freni, L. Spadaro, V. Chiodo, G. Bonura, S. Donato, S. Cavallaro, Catal. Commun. 5 (2004) 611–615.
[9] S. Arndt, G. Laugel, S. Levchenko, R. Horn, M. Baerns, M. Scheffler, R. Schlögl, R. Schomäcker, Catal. Rev. Sci. Eng. 53 (2011) 424–514.
[10] P.W. Tasker, J. Phys. C: Solid State Phys. 12 (1979) 4977–4984.
[11] A. Wander, I.J. Bush, N.M. Harrison, Phys. Rev. B 68 (2003) 233405.
[12] C. Duriez, C. Chapon, C.R. Henry, J.M. Rickard, Surf. Sci. 230 (1990) 123–136.
[13] Y. Yan, M.F. Chisholm, S.J. Pennycook, S.T. Pantelides, Surf. Sci. 442 (1999) 251–255.
[14] N.V. Skorodumova, K. Hermansson, B. Johansson, Phys. Rev. B 72 (2005) 125414.
[15] C.R. Henry, Surf. Sci. Rep. 31 (1998) 235–325.
[16] C. Barth, C.R. Henry, Phys. Rev. Lett. 91 (2003) 196102.
[17] G. Pacchioni, in: U. Heiz, U. Landman (Eds.), Nanocatalysis. Nanoscience and Technology, Springer, Berlin, Heidelberg, 2007, pp. 193–243.
[18] G. Pacchioni, H. Freund, Chem. Rev. 113 (2013) 4035–4072.
[19] A. Sanchez, S. Abbet, U. Heiz, W.-D. Schneider, H. Häkkinen, R.N. Barnett, U. Landman, J. Phys. Chem. 103 (1999) 9573–9578.
[20] S. Abbet, A. Sanchez, U. Heiz, W.D. Schneider, A.M. Ferrari, G. Pacchioni, N. Rosch, J. Am. Chem. Soc. 122 (2000) 3453–3457.
[21] S. Abbet, A. Sanchez, U. Heiz, W.-D. Schneider, J. Catal. 198 (2001) 122–127.
[22] S. Recchia, C. Dossi, N. Poli, A. Fusi, L. Sordelli, R. Psaro, J. Catal. 184 (1999) 1–4.
[23] I. Kikuchi, Y. Haibara, M.-A. Ohshima, H. Kurokawa, H. Miura, J. Jpn. Pet. Inst. 55 (2012) 33–39.
[24] A. Virnovskaia, S. Morandi, E. Rytter, G. Ghiotti, U. Olsbye, J. Phys. Chem. C 111 (2007) 14732–14742.
[25] V. Ponec, Appl. Catal., A 149 (1997) 27–48.
[26] Y. Jugnet, R. Sedrati, J.C. Bertolini, J. Catal. 229 (2005) 252–258.
[27] C. Xu, J.W. Peck, B.E. Keel, J. Am. Chem. Soc. 115 (1993) 751–755.
[28] G. Stalnionis, L. Tamasauskaite-Tamasiunaite, V. Pautieniene, Z. Jusys, J. Solid State Electrochem. 8 (2004) 900–907.
[29] W. Koch, M.C. Holthausen, A Chemist's Guide to Density Functional Theory, Second ed., Wiley-VCH Verlag GmbH, Weinheim, Germany, 2001.

[30] I. Yudanov, G. Pacchioni, K. Neyman, N. Rösch, J. Phys. Chem. B 101 (1997) 2786–2792.
[31] A.M. Ferrari, G. Pacchioni, J. Phys. Chem. 100 (1996) 9032–9037.
[32] N. López, F. Illas, J. Phys. Chem. B 102 (1998) 1430–1436.
[33] A. Bogicevic, D.R. Jennison, Surf. Sci. 437 (1999) L741–L747.
[34] N. Lopez, J. Chem. Phys. 114 (2001) 2355–2361.
[35] N. Lopez, J.C. Paniagua, F. Illas, J. Chem. Phys. 117 (2002) 9445–9451.
[36] A. Markovits, J.C. Paniagua, N. Lopez, C. Minot, F. Illas, Phys. Rev. B 67 (2003) 115417.
[37] K.M. Neyman, C. Inntam, V.A. Nasluzov, R. Kosarev, N. Rösch, Appl. Phys. A 78 (2004) 823–828.
[38] J.R.B. Gomes, F. Illas, B. Silvi, Chem. Phys. Lett. 388 (2004) 132–138.
[39] Y. Wang, E. Florez, F. Mondragon, T.N. Truong, Surf. Sci. 600 (2006) 1703–1713.
[40] Y. Su, Y. Wang, G. Chen, T.N. Truong, J. Theor. Comput. Chem. 8 (2009) 1155–1169.
[41] W.S. Abdel Halim, A.S. Shalabi, K.A. Soliman, Int. J. Quantum Chem. 109 (2009) 1094–1102.
[42] A.S. Shalabi, W.S. Abdel Halim, M.S. Ghonaim, Physica B 406 (2011) 397–405.
[43] A.S. Shalabi, S. Abdel Aal, W.S. Abdel Halim, M.S. Ghonaim, Int. J. Quantum Chem. 111 (2011) 2444–2453.
[44] T. Mineva, V. Alexiev, C. Lacaze-Dufaure, E. Sicilia, C. Mijoule, N. Russo, J. Mol. Struct. Theochem. 903 (2009) 59–66.
[45] K. Honkala, H. Hakkinen, J. Phys. Chem. C 111 (2007) 4319–4327.
[46] J.C. Lian, E. Finazzi, C. Di Valentin, T. Risse, H.-J. Gao, G. Pacchioni, H.-J. Freund, Chem. Phys. Lett. 450 (2008) 308–311.
[47] J. Zhu, J.A. Farmer, N. Ruzycki, L. Xu, C.T. Campbell, G. Henkelman, J. Am. Chem. Soc. 130 (2008) 2314–2322.
[48] T. Makino, S.I. Tanaka, Adv. Mater. Res. 11–12 (2006) 485–488.
[49] Y. Zhao, B. Teng, Z. Yang, Y. Zhao, L. Zhao, M. Luo, J. Phys. Chem. C 115 (2011) 16461–16466.
[50] X. Sun, S.D. Li, B. Wang, M. Kurahashi, A. Pratt, Y. Yamauchi, Phys. Chem. Chem. Phys. 16 (2014) 95–102.
[51] H. Gao, Chem. Phys. Lett. 657 (2016) 11–17.
[52] A.D. Becke, J. Chem. Phys. 98 (1993) 5648–5652.
[53] S.H. Vosko, L. Wilk, M. Nusair, Can. J. Phys. 58 (1980) 1200–1211.
[54] C. Lee, W. Yang, R.G. Parr, Phys. Rev. B 37 (1988) 785–789.
[55] S. Grimme, J. Antony, S. Ehrlich, H. Krieg, J. Chem. Phys. 132 (2010) 154104.
[56] S. Grimme, S. Ehrlich, L. Goerigk, J. Comput. Chem. 32 (2011) 1456–1465.
[57] Z. Huesges, C. Müller, B. Paulus, L. Maschio, Surf. Sci. 627 (2014) 11–15.
[58] W.J. Hehre, R. Ditchfield, J.A. Pople, J. Chem. Phys. 56 (1972) 2257–2261.
[59] M.M. Francl, W.J. Pietro, W.J. Hehre, J.S. Binkley, M.S. Gordon, D.J. DeFrees, J.A. Pople, J. Chem. Phys. 77 (1982) 3654–3665.
[60] T. Clark, J. Chandrasekhar, G.W. Spitznagel, P.V.R. Schleyer, J. Comput. Chem. 4 (1983) 294–301.
[61] S.A. Fuente, P.G. Belelli, R.M. Ferullo, N.J. Castellani, Surf. Sci. 602 (2008) 1669–1676.
[62] S.A. Fuente, P.G. Belelli, M.M. Branda, R.M. Ferullo, N.J. Castellani, Appl. Surf. Sci. 255 (2009) 7380–7384.
[63] K.M. Eid, H.Y. Ammar, Appl. Surf. Sci. 258 (2012) 7689–7698.
[64] W.R. Wadt, P.J. Hay, J. Chem. Phys. 82 (1985) 284–298.
[65] L.E. Roy, P.J. Hay, R.L. Martin, J. Chem. Theory Comput. 4 (2008) 1029–1031.
[66] C.E. Check, T.O. Faust, J.M. Bailey, B.J. Wright, T.M. Gilbert, L.S. Sunderlin, J. Phys. Chem. A 105 (2001) 8111–8116.
[67] S.F. Boys, F. Bernardi, Mol. Phys. 19 (1970) 553–566.
[68] R.F.W. Bader, Atoms in Molecules: a Quantum Theory, Clarendon, Oxford, UK, 1990.
[69] M.J. Frisch, G.W. Trucks, H.B. Schlegel, G.E. Scuseria, M.A. Robb, J.R. Cheeseman, G. Scalmani, V. Barone, B. Mennucci, G.A. Petersson, H. Nakatsuji, M. Caricato, X. Li, H.P. Hratchian, A.F. Izmaylov, J. Bloino, G. Zheng, J.L. Sonnenberg, M. Hada, M. Ehara, K. Toyota, R. Fukuda, J. Hasegawa, M. Ishida, T. Nakajima, Y. Honda, O. Kitao, H. Nakai, T. Vreven, J.A. Montgomery Jr., J.E. Peralta, F. Ogliaro, M. Bearpark, J.J. Heyd, E. Brothers, K.N. Kudin, V.N. Staroverov, T. Keith, R. Kobayashi, J. Normand, K. Raghavachari, A. Rendell, J.C. Burant, S.S. Iyengar, J. Tomasi, M. Cossi, N. Rega, J.M. Millam, M. Klene, J.E. Knox, J.B. Cross, V. Bakken, C. Adamo, J. Jaramillo, R. Gomperts, R.E. Stratmann, O. Yazyev, A.J. Austin, R. Cammi, C. Pomelli, J.W. Ochterski, R.L. Martin, K. Morokuma, V.G. Zakrzewski, G.A. Voth, P. Salvador, J.J. Dannenberg, S. Dapprich, A.D. Daniels, O. Farkas, J.B. Foresman, J.V. Ortiz, J. Cioslowski, D.J. Fox, Gaussian 09 D.01, Gaussian, Inc., Wallingford CT, 2013.
[70] T. Lu, F. Chen, J. Comput. Chem. 33 (2012) 580–592.
[71] Y. Li, D.C. Langreth, M.R. Pederson, Phys. Rev. B 52 (1995) 6067–6080.
[72] S. Fernandez, A. Markovits, F. Fuster, C. Minot, J. Phys. Chem. C 111 (2007) 6781–6788.
[73] S. Fernandez, A. Markovits, C. Minot, Chem. Phys. Lett. 463 (2008) 106–111.
[74] A.M. Ferrari, G. Pacchioni, J. Phys. Chem. 99 (1995) 17010–17018.
[75] M. Sterrer, E. Fischbach, M. Heyde, N. Nilius, H.-P. Rust, T. Risse, H.-J. Freund, J. Phys. Chem. B 110 (2006) 8665–8669.
[76] J. Kramer, W. Ernst, C. Tegenkamp, H. Pfnur, Surf. Sci. 517 (2002) 87–97.
[77] P. Baranek, G. Pinarello, C. Pisani, R. Dovesi, Phys. Chem. Chem. Phys. 2 (2000) 3893–3901.
[78] M. Sterrer, T. Risse, U.M. Pozzoni, L. Giordano, M. Heyde, H.-P. Rust, G. Pacchioni, H.-J. Freund, Phys. Rev. Lett. 98 (2007) 096107.
[79] D.M. Popolan, M. Nössler, R. Mitrić, T.M. Bernhardt, V. Bonačić-Koutecký, J. Phys. Chem. A 115 (2011) 951–959.
[80] D.R. Kauffman, D. Alfonso, C. Matranga, P. Ohodnicki, X. Deng, R.C. Siva, C. Zeng, R. Jin, Chem. Sci. 5 (2014) 3151–3157.